First publ. in: Biochemistry 27 (1988), 17, pp. 6599-6611

Oxidation–Reduction of General Acyl-CoA Dehydrogenase by the Butyryl-CoA/Crotonyl-CoA Couple. A New Investigation of the Rapid Reaction Kinetics†

Lawrence M. Schopfer* and Vincent Massey

Department of Biological Chemistry, The University of Michigan Medical School, Ann Arbor, Michigan 48109-0606

Sandro Ghisla

Fakultät Biologie, Universität Konstanz, D7750 Konstanz, West Germany

Colin Thorpe

Department of Chemistry, University of Delaware, Newark, Delaware 19716

ABSTRACT: Pig kidney general acyl-CoA dehydrogenase (GAD) can be reduced by butyryl-CoA to form reduced enzyme and crotonyl-CoA. This reaction is reversible. Stopped-flow, kinetic investigations on GAD have been made, using the following reaction pairs: oxidized GAD/butyryl-CoA, oxidized GAD/crotonyl-CoA, oxidized GAD/α,β-dideuteriobutyryl-CoA, reduced GAD/butyryl-CoA, and reduced GAD/crotonyl-CoA (in 50 mM potassium phosphate buffer, pH 7.6 at 4 °C). Reduction of GAD by butyryl-CoA is triphasic. The slowest phase is 100-fold slower than the preceding phase and appears to represent a secondary process not directly related to the primary reduction events. The first two fast phases are responsible for reduction of GAD. Reduction proceeds via a reduced enzyme/crotonyl-CoA charge-transfer complex. α,β-Dideuteriobutyryl-CoA elicits a major deuterium isotope effect (15-fold) on the reduction reaction. Oxidation of GAD by crotonyl-CoA is biphasic. Oxidation proceeds via the same reduced enzyme/crotonyl-CoA charge-transfer complex seen during reduction. The oxidation reaction ends in a mixture composed largely of oxidized GAD species. From the data, we constructed a mechanism for the reduction/oxidation of GAD by butyryl-CoA/crotonyl-CoA. This mechanism was then used to simulate all of the observed kinetic time course data, using a single set of kinetic parameters. A close correspondence between the observed and simulated data was obtained.

General acyl-CoA dehydrogenase (GAD)[1] is a flavoenzyme that catalyzes the first step in fatty acid β-oxidation. This involves the insertion of a trans double bond between C-2 and C-3 of its fatty acyl thioester. GAD was isolated from pig liver mitochondria and characterized by Beinert and co-workers in the late 1950s (Crane et al., 1956; Hauge, 1956; Beinert & Page, 1957; Steyn-Parvé & Beinert, 1958; Beinert, 1962; Beinert & Sands, 1961). In the last 10 years, it has become the subject of investigation in several laboratories. Enzyme from pig liver (Crane et al., 1956; Hall & Kamin, 1975), pig kidney (Thorpe et al., 1979), bovine liver (Dommes & Kunau, 1984; Murfin, 1974), bovine heart (Beinert, 1962; Davidson & Schultz, 1982), and rat liver (Ikeda et al., 1985a; Furuta et al., 1981) has been studied. Therefore, a certain variability can be found in the primary observations. However, a number of general mechanistic features of GAD have been established.

First, reduction of GAD by acyl-CoA yields a long-wavelength species. The structure of this species has been a matter of considerable interest, over which there is still some dispute. It has been described as a charge-transfer complex in which reduced GAD is the donor and enoyl-CoA is the acceptor on the basis of (1) the absence of an EPR signal for the complex (Beinert & Sands, 1961; Hall et al., 1979), which argues against semiquinone involvement, (2) shifting of the long-wavelength peak position in response to changing the substrate (Murfin, 1974; Reinsch et al., 1980) or the flavin (Thorpe & Massey, 1983), which is characteristic of charge-transfer interactions, (3) an absorbance spectrum that is markedly different from either the neutral (Thorpe et al., 1979) or anionic (Mizzer & Thorpe, 1981) semiquinones of GAD, again implying the noninvolvement of semiquinones, (4) the extensive bleaching of the 450-nm chromophore that occurs concomitant with the appearance of the long-wavelength band (Beinert & Page, 1957; Hall et al., 1979), which suggests reduction of the flavin, and (5) the appearance of the spectrum of enoyl-CoA in parallel with the formation of the long-wavelength band when β-2-furylpropionyl-CoA is used as substrate (McFarland et al., 1982), which indicates oxidation of the substrate. However, arguments have been made to the effect that the flavin is not reduced in this long-wavelength intermediate. It has been suggested that the intermediate could be a "resonance hybrid" involving oxidized flavin, the acyl-CoA carbanion, and a mutually shared hydride ion (Ikeda et al., 1985b).

Next, the amplitude of the long-wavelength band is dependent on the chain length of the acyl-CoA reductant (Thorpe et al., 1979; Hall et al., 1979; Ikeda et al., 1985b). Steady-state activity is also related to the acyl-CoA chain length (Hauge, 1956; Dommes & Kunau, 1984; Davidson & Schultz, 1982; Furuta et al., 1981; Hall et al., 1979; Ikeda et al., 1985c) and

† This work was supported by National Institutes of Health Grants GM-11106 (V.M.) and GM-26643 (C.T.) and by a grant from the Deutsche Forschungsgemeinschaft (Gh 2/4-5 to S.G.).

* Author to whom correspondence should be addressed.

[1] Abbreviations: GAD, general acyl-CoA dehydrogenase; B-CoA, butyryl-CoA; C-CoA, crotonyl-CoA.

can be correlated with the amplitude of this absorbance band (Hall et al., 1979; Ikeda et al., 1985c). This long-wavelength complex has been shown to be the donor for the physiological electron acceptor, electron-transferring flavoprotein (Hall & Lambeth, 1980; Gorelick et al., 1985).

Finally, GAD reduction is initiated by GAD-mediated abstraction of the C-2 proton from the acyl-CoA reductant. This is indicated by (1) GAD-mediated exchange of the substrate C-2 proton for deuterium in the medium (Ghisla et al., 1984; Ikeda et al., 1985b), (2) activation of mechanism-based inhibitors (Wenz et al., 1981, 1985; Frerman et al., 1980), and (3) reactivity of acyl-CoA analogues with GAD (Thorpe et al., 1981). Transfer of a hydride equivalent from C-3 of the acyl-CoA to N-5 of the isoalloxazine (Ghisla et al., 1984) occurs in a concerted manner with the C-2 proton abstraction (Pohl et al., 1986).

The manner in which GAD modulates the chemistry to alter the levels and stability of the long-wavelength intermediate is not well understood. We have used rapid reaction kinetics to examine the reactions of butyryl-CoA with oxidized and reduced GAD as well as the reactions of crotonyl-CoA with oxidized and reduced GAD. From the data, we have constructed a mechanism that satisfactorily encompasses all the rapid reaction data, including the multiphasic behavior seen with certain substrates, and provides a useful basis for rationalizing some of the unresolved issues concerning the behavior of GAD. Our data support the charge-transfer assignment for the long-wavelength intermediate, wherein reduced FAD is the donor and crotonyl-CoA is the acceptor.

Experimental Procedures

Materials

General acyl-CoA dehydrogenase (EC 1.3.99.3) was purified from pig kidney as previously described (Thorpe et al., 1979) and stored at −20 °C. The GAD concentration was determined spectrophotometrically with an extinction coefficient for the oxidized enzyme of 15.4 mM^{-1} cm^{-1} at 446 nm (Thorpe et al., 1979). All GAD concentrations refer to the concentration of flavin, i.e., active sites.

Crotonase (bovine liver), butyryl-CoA (lithium salt), and crotonyl-CoA (lithium salt) were purchased from Sigma Chemical Co. The α,β-dideuteriobutyryl-CoA was synthesized as previously described (Ghisla et al., 1984). All other chemicals were of reagent grade and were used without additional purification.

Methods

Spectra and the "slow-phase" kinetics were recorded with a Cary Model 219 double-beam spectrophotometer, with temperature-controlled cell holders. All reactions were performed in 50 mM potassium phosphate buffer, pH 7.6 at 4 °C, unless otherwise indicated.

Anaerobic Technique. Anaerobic enzyme samples were prepared in an all-glass apparatus (Williams et al., 1979) by sequential evacuation and reequilibration with oxygen-free nitrogen. Prepurified nitrogen was passed over a heated column of Ridox (Fischer Chemical Co.) to remove traces of oxygen. Reagents were made anaerobic by bubbling oxygen-free nitrogen through them for 15 min in Luer-tipped syringes.

Rapid Reaction. Rapid reaction absorbance measurements were made in a temperature-controlled, anaerobic stopped-flow apparatus interfaced to a Nova II (Data General) computer (Beaty & Ballou, 1981). A cutoff filter (Wratten No. 15) was used for measurements at wavelengths greater than 530 nm, to avoid stray light. When used in its spectrum mode, the stopped-flow apparatus is capable of scanning at 60 nm s^{-1}.

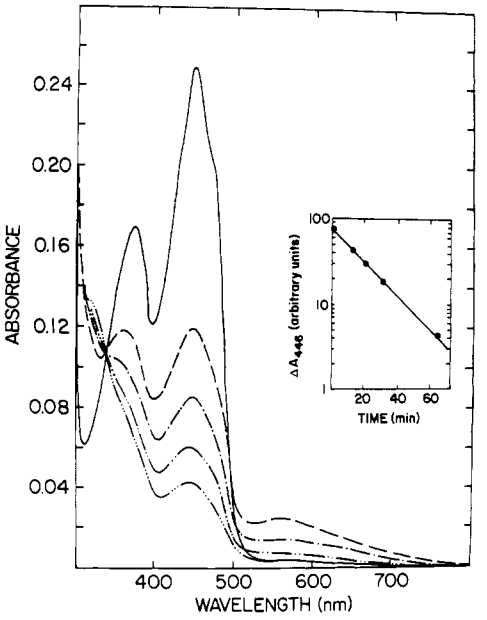

FIGURE 1: Spectra of the slow phase in the reduction of oxidized GAD by butyryl-CoA. Conditions: oxidized GAD (16.2 μM) was anaerobically mixed with butyryl-CoA (67 μM) in 50 mM potassium phosphate buffer, pH 7.6 at 4 °C. Spectra were taken in a Cary 219 spectrophotometer before mixing (solid line), immediately after mixing (dashed line), after 10 min (dash-dot line), after 29 min (dash-dot-dot line), and at the end of the reaction (dash-dot-dot-dot line). The scan rate was 2 nm s^{-1}. Some traces have been omitted for clarity. Inset: The half-life of the slow phase ($t_{1/2}$ = 16 min) was calculated from a plot of the logrithum of the difference (time point minus final) in absorbance at 446 nm versus time. Time 0 represents the end of the fast phases, i.e., the dashed line curve.

Reduced GAD was prepared by visible light irradiation in the presence of 5-deazaflavin (1 μM) and EDTA (10 mM) (Massey & Hemmerich, 1978).

Simulations. The rapid reaction data were simulated on a Nova II computer by using a fourth-order Runge–Kutta numerical method (Forsythe et al., 1977) to solve the set of differential equations that described our chosen mechanism. The mechanism was selected on the basis of a qualitative analysis of the rate data, as described under Results. Initial estimates for the rate constants and extinction coefficients used in the simulation were taken from a quantitative analysis of the rate data, as described under Results. These initial estimates were then adjusted by trial and error until a "best fit" between simulated and measured results was obtained.

Results

Mixing butyryl-CoA with oxidized GAD (in 50 mM potassium phosphate, pH 7.6, 4 °C) resulted in a triphasic reaction. There was an initial, rapid portion, which consisted of two phases. Both phases were complete by 40 s (Figure 1, dashed line). During this period, the spectrum of the enzyme underwent a loss of absorbance in the 340–500-nm region and a rise in both the 500–800-nm (peak ~550 nm) and 300–340-nm regions. The third phase lasted for ~2 h ($t_{1/2}$ = 16 min). The spectral changes in this phase were isobestic at 342 nm, consisting of a general bleaching from 342 to 800 nm and a rise from 300 to 342 nm. The spectrum taken at the end point of this triphasic sequence (Figure 1, dash-dot-dot-dot line) is different from that of reduced GAD obtained by dithionite or EDTA/5-deazaflavin/light reduction (Beinert & Page, 1957; Thorpe et al., 1979) (Figure 5, dotted line). However, it is similar to the spectra of reduced GAD/ligand complexes (Figure 5, open circles and closed squares) or oc-

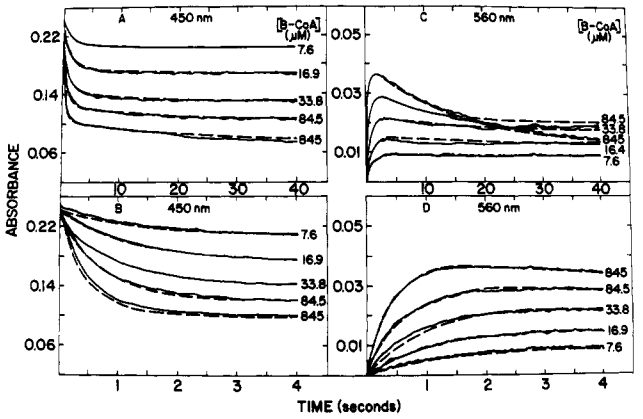

FIGURE 2: Rapid phases in the reduction of oxidized GAD by butyryl-CoA. Conditions: oxidized GAD (16.4 μM) was anaerobically mixed with butyryl-CoA (15.2–1690 μM) in 50 mM potassium phosphate buffer, pH 7.6 at 4 °C, with a stopped-flow spectrophotometer (2-cm optical path length). The panels show the time course of the reaction: (A) at 450 nm, over 40 s; (B) at 450 nm, over 4 s; (C) at 560 nm, over 40 s; (D) at 560 nm, over 4 s. The concentrations of butyryl-CoA (B-CoA) after mixing are indicated opposite each trace. The solid lines are the measured time courses. The dashed lines are simulations based on the scheme in eq 4, using the parameters in Tables I and II.

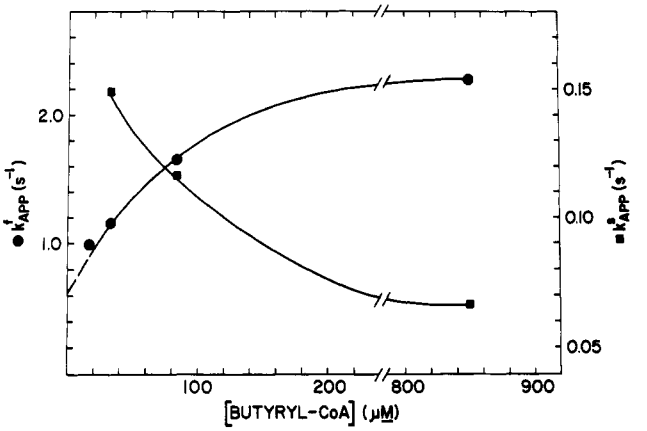

FIGURE 3: Plot of the apparent rate (k^f_{app} and k^s_{app}, f = fast phase and s = slow phase) for both of the rapid phases versus the concentration of butyryl-CoA. Conditions: same as in Figure 2. The Y-axis scale for the solid circles is on the left, and the Y-axis scale for the solid squares is on the right. The points each represent an average of five measurements.

tanoyl-CoA/reduced GAD (Beinert & Page, 1957; Thorpe et al., 1979; Hall et al., 1979; Ikeda et al., 1985c; Auer & Frerman, 1980). We therefore propose that the end point of the slow phase is a ligand complex of fully reduced GAD.

The Slow Phase. In order to analyze this sequence of events, we feel that the third, slow phase should be separated from the first two phases. The most obvious reason for this is the great difference in observed rates. It seems reasonable to suggest that the events occurring in the fast phases have reached completion before the slow phase has effectively begun. From this vantage, the third phase can be viewed as a secondary process. It is important to note that the slow phase is seen only with butyryl-CoA and not with octanoyl-CoA or palmitoyl-CoA (Beinert & Page, 1957).

Though we will not be including this slow phase in our considerations, we have investigated its behavior under a variety of conditions. We found that the rate of the slow phase was independent of butyryl-CoA concentration (15–410 μM), oxygen concentration (anaerobic versus air saturation), and phosphate buffer concentration (5 mM–1 M). In addition, fractional release of crotonyl-CoA from the enzyme occurred during the fast phases, but no release occurred during the slow phase. Finally, addition of crotonase to the reaction did not accelerate the rate.

Summarizing these experiments, we can suggest that the slow phase is a process that is separate from the fast phases. It is not associated with slow product release, and the conversion of free crotonyl-CoA to β-hydroxybutyryl-CoA by the crotonase activity, present in GAD preparations (Lau et al., 1986), is not involved. Though we have not identified the cause of the slow phase, we will now address the fast phases observed in the reaction of butyryl-CoA with oxidized GAD as a separate issue.

Fast Phases: Reduction of Oxidized GAD by Butyryl-CoA. Mixing oxidized GAD (16.4 μM) with an equal volume of buffer containing excess butyryl-CoA (anaerobically) in the stopped-flow spectrophotometer resulted in a biphasic decrease in absorbance at 450 nm and an increase followed by a decrease in absorbance at 560 nm (Figure 2, panels A–D). The observations at 560 nm are critical to the interpretation of the mechanism. Formation of 560-nm absorbance followed by its partial decay argues that the two phases in this reaction represent the formation of a species followed by its decay to an equilibrium level. An interpretation such as this is not possible from the 450-nm traces alone. The rise and fall in absorbance at 560 nm is also incompatible with earlier suggestions (Reinsch et al., 1980) that the biphasic kinetics represented two populations of enzyme, each reacting at a different rate. These earlier workers came to their conclusions largely on the basis of finding a biphasic reaction at 450 nm and only a monophasic reaction at 560 nm (pH 6.6 and pH 8.6) (Reinsch et al., 1980, 1983). We have repeated the above reaction at pH 8.5 and pH 6.1 (4 °C) and at pH 7.6 (25 °C). In all instances, we saw a biphasic reaction at both 450 and 560 nm. We have no explanation for this discrepancy.

As the concentration of butyryl-CoA was increased, the end point of the reaction tended toward greater bleaching at 450 nm, a sign of increased reduction. In the presence of 845 μM butyryl-CoA, 68% of the initial 450-nm absorbance was lost. The 560-nm traces were slightly more complex. At 3 s (the time of maximum absorbance at 560 nm), the absorbance increased as the concentration of butyryl-CoA was increased. But the position of the final absorbance (40 s after mixing) did not follow this pattern. As the butyryl-CoA concentration was increased, up to 85 μM, there was a steady rise in the absorbance. However, at 845 μM butyryl-CoA, the final long-wavelength absorbance was back down to about the same level as that for 16 μM butyryl-CoA (Figure 2, panel C).

These results indicate that butyryl-CoA reduces GAD to an equilibrium position in the fast phases and that reduction involves at least one intermediate. The intermediate exhibits long-wavelength absorbance and can be present in significant amounts at equilibrium. The equilibrium, however, is not simple. The level of the final absorbance at 560 nm is first increased and then decreased by increasing the butyryl-CoA concentration. This finding suggests that butyryl-CoA enters into the reaction more than once.

The apparent rate of the fast phase (k^f_{app}) showed a slight increase, leading to saturation, as the concentration of butyryl-CoA was increased (Figure 3). The apparent rate of the slower phase (k^s_{app}) showed an unusual decrease as the butyryl-CoA concentration was increased (Figure 3). Similar observations have been made for this reaction by other groups (Hall et al., 1979; Reinsch et al., 1980; Pohl et al., 1986). Such corroboration is important since the substrate dependencies are small and might be dismissed as experimental error if they

did not appear repeatedly in the work from different laboratories. Measured rates for each phase were the same at both 560 and 450 nm. The substrate dependencies being of qualitatively different types for the two observed rates suggests that butyryl-CoA enters the mechanism twice. The substrate dependence data do not however provide an unequivocal basis for assigning the order in which the rates appear in the mechanism.

Ordering of the events can be made on the basis of the amplitude of the transient intermediate seen at 560 nm (Alcock et al., 1970). The fully developed spectrum of this intermediate was obtained, transiently, by reacting reduced GAD with crotonyl-CoA (see below). The maximum amplitude at 560 nm in the reductive time course (Figure 2, panel C: 845 μM butyryl-CoA) is close to the absorbance amplitude seen for the fully developed intermediate. This argues strongly that k^f_{app} accompanies formation of the intermediate and k^s_{app} accompanies its decay. Were the order of the rates reversed, the maximum amount of intermediate observed would be much less than the actual maximum. From Figure 2, panels A and C, it can be seen that the absorbance rise at 560 nm is associated with substantial bleaching of the flavin chromophore, especially at 845 μM butyryl-CoA. This indicates that reduction of the flavin is concomitant with the formation of the intermediate.

The saturating substrate dependence of k^f_{app} suggests eq 1 as a minimum scheme for the formation of the long-wavelength intermediate. GAD_o is oxidized GAD, B-CoA is butyryl-CoA,

$$GAD_o + \text{B-CoA} \overset{K_{d_1}}{\leftrightarrow} MC_1 \underset{k_{-1}}{\overset{k_1}{\rightleftharpoons}} I \qquad (1)$$

MC_1 is a Michaelis–Menten complex between oxidized GAD and butyryl-CoA, and I is the long-wavelength, reduced enzyme intermediate. Formation of MC_1 can be seen spectrally if perdeuteriobutyryl-CoA is used as the reductant (Pohl et al., 1986). The reversibility of this scheme is not apparent from the substrate-dependence information. It is taken from the overall reversibility of this reaction, which will be developed later. Reversibility for this portion of the reaction has been suggested on the basis of steady-state and stopped-flow kinetics (Thorpe et al., 1981; Pohl et al., 1986). The value of k_{-1} can be estimated to be $\sim$0.6 s^{-1} from the Y-axis intercept of Figure 3 (Strickland et al., 1975). The sum $(k_1 + k_{-1})$ can be estimated to be $\sim$2.3 s^{-1} from the saturation limit. By difference, k_1 becomes $\sim$1.7 s^{-1}. Using $k_{-1} = 0.6$ s^{-1}, a plot of $1/(k^f_{app} - k_{-1})$ versus 1/[butyryl-CoA] gave a straight line with a nonzero intercept (data not shown) from which K_{d_1} could be estimated to be 37 μM (Strickland et al., 1975).

The negative dependence of k^s_{app} on butyryl-CoA concentration is quite informative. The only simple mechanism that can account for such a substrate dependence is shown in eq 2. I is the same intermediate as in eq 1. X is a form of

$$I \underset{k_{-2}}{\overset{k_2}{\rightleftharpoons}} X \underset{k_{-3}}{\overset{[\text{B-CoA}]\cdot k_3}{\rightleftharpoons}} X\cdot\text{B-CoA} \qquad (2)$$

reduced enzyme, which will be identified later. The substrate, B-CoA, enters the reaction a second time by combining with species X.

A model of this form has been used by Kirschner et al. and Halford to account for the negative dependence of apparent rate on ligand concentration for situations in which there is a rapid binding of ligands to proteins that exist in two, slowly interconvertible forms (Kirschner et al., 1966; Halford, 1972). In this Kirschner/Halford situation, the limiting rate at low ligand concentration is $k_2 + k_{-2}$, while the limiting rate at high ligand concentration is k_2. As will be seen below, this combination of limiting rates does not satisfy our data. We have, however, found an alternate situation (still based on eq 2) that also predicts a negative dependence of observed rate on ligand concentration and fits our data. Our treatment is developed in the Appendix, part A. In our situation, k_2 is the limit at high ligand concentration and k_{-3} is the limit at low ligand concentration. On the basis of our analysis, the data in Figure 3 indicate a value of $\sim$0.07 s^{-1} for k_2 and 0.15 s^{-1} for k_{-3}. Establishing values for k_{-2} and k_3 requires additional information, which will be presented below.

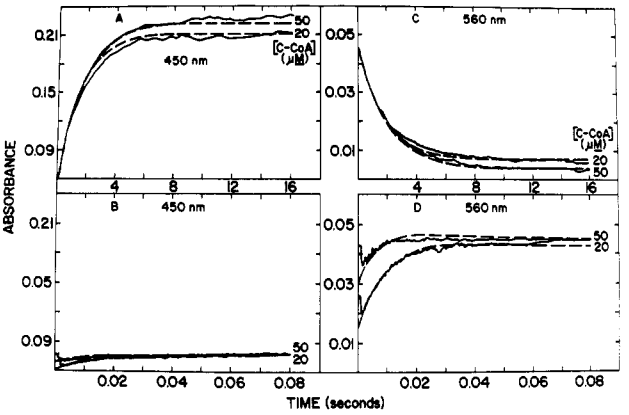

FIGURE 4: Oxidation of reduced GAD by crotonyl-CoA. Conditions: reduced GAD (16.2 μM) was anaerobically mixed with crotonyl-CoA (40 and 100 μM) in 50 mM potassium phosphate buffer, pH 7.6 at 4 °C, with a stopped-flow spectrophotometer (2-cm optical path length). The panels show the time course of the reaction: (A) at 450 nm, over 16 s; (B) at 450 nm, over 0.08 s; (C) at 560 nm, over 16 s; (D) at 560 nm, over 0.08 s. The concentrations of crotonyl-CoA (C-CoA) after mixing are indicated opposite each trace. The solid lines are the measured time courses. The dashed lines are simulations based on the scheme in eq 4, using the parameters in Tables I and II.

Oxidation of Reduced GAD with Crotonyl-CoA. Mixing 16.2 μM reduced GAD with an equal volume of buffer containing excess crotonyl-CoA (anaerobically) in the stopped-flow spectrophotometer resulted in a biphasic reaction (Figure 4). At 450 nm, there was a small rise over 80 ms, followed by a large rise over 16 s. At 560 nm, there was a fast rise, followed by a slow fall. The apparent rate of the fast phase increased from 117 s^{-1} at 20 μM crotonyl-CoA to 214 s^{-1} at 50 μM crotonyl-CoA. At yet higher concentrations of crotonyl-CoA, the reaction was complete in the dead time of the stopped-flow apparatus. The apparent rate of the slow phase was essentially independent of the crotonyl-CoA concentration, measuring 0.5 s^{-1}. From this substrate-dependence data, we argue that the fast phase involves formation of the long-wavelength intermediate and the slow phase its decay. There is not enough information in the fast-phase data to discriminate between a second-order formation of the intermediate and a mechanism involving the formation of a Michaelis–Menten complex prior to the intermediate.

On the basis of the large difference in rates between the fast and slow phases, it is reasonable to suggest that the intermediate is fully formed by 80 ms. Thus, it is possible to reconstruct a spectrum of the intermediate by plotting the absorbance at 80 ms (measured relative to the final spectrum) for a series of wavelengths. The conditions of the reaction are described in the legend to Figure 5. We used as a final reference spectrum the spectrum of the reaction mixture taken in the stopped-flow spectrophotometer after 2 min, when all the absorbance changes had stopped. This gave us an accurate, empirical reference. From Figure 5, it can be seen that the final spectrum is a mixture of oxidized GAD species plus a

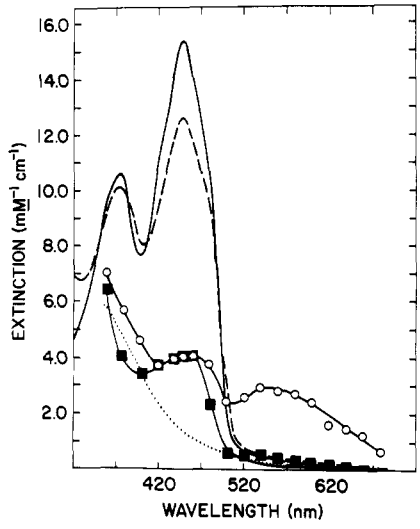

FIGURE 5: Spectra of the various species appearing during the oxidation of reduced GAD by crotonyl-CoA. Conditions: reduced GAD (16.2 μM) was anaerobically mixed with crotonyl-CoA (100 μM) in 50 mM potassium phosphate buffer, pH 7.6 at 4 °C, with a stopped-flow spectrophotometer (2-cm optical path length). Spectra: initial oxidized GAD (solid line); photoreduced GAD (dotted line); species immediately after mixing (closed squares); long-wavelength intermediate I, measured 80 ms after mixing (open circles); final, stable reaction mixture (dashed line). Spectra marked by symbols were constructed from the stopped-flow time traces. The symbols indicate the wavelengths at which measurements were actually made.

fraction of the long-wavelength intermediate. Finding oxidized GAD as a product of the reaction of reduced GAD and crotonyl-CoA establishes that the overall reaction is reversible, as written in eq 1 and 2. That the full spectrum of free oxidized GAD is not obtained indicates that the reverse reaction ends at an equilibrium state. These observations are contrary to results reported by Reinsch et al. (1980). No obvious reason for the difference is available.

The spectrum of the intermediate (I) (also given in Figure 5) shows it to be a reduced flavin species, on the basis of the low absorbance in the 450-nm region. The long-wavelength band has a maximum at 540–560 nm with an extinction coefficient of 2.8 mM^{-1} cm^{-1}. The shape of the intermediate spectrum is different from that of either the neutral or anionic semiquinone spectra of GAD (Thorpe et al., 1979; Mizzer & Thorpe, 1981). On the basis of these observations, we support the view (Murfin, 1974; Reinsch et al., 1980; Thorpe & Massey, 1983) that the intermediate is a charge-transfer complex with reduced GAD as the donor and crotonyl-CoA as the acceptor.

The reaction conditions used to resolve the intermediate resulted in a formation rate that was so fast that about three-fourths of the absorbance change, at 560 nm, occurred in the dead time of the stopped-flow apparatus. This can be seen in Figure 4, panel D (50 μM crotonyl-CoA trace). In order to estimate the spectrum of the enzyme immediately after mixing, we therefore multiplied the observed fast-phase absorbance change by 4 and subtracted that value from the intermediate spectrum. As can be seen in Figure 5, the resultant spectrum is not that of reduced GAD. The increased absorbance in the 450-nm region strongly suggests that crotonyl-CoA has already bound to reduced GAD, causing a spectral perturbation. An absorbance increase in this region also occurred when butyryl-CoA was mixed anaerobically with reduced GAD (see below). We conclude, therefore, that reaction of crotonyl-CoA with reduced GAD to form the long-wavelength species proceeds via the formation of a Michaelis–Menten complex.

An overall scheme for the oxidation of reduced GAD by crotonyl-CoA is given in eq 3. GAD_r is reduced GAD, C-CoA

$$GAD_r + \text{C-CoA} \overset{K_{d_2}}{\leftrightarrow} MC_2 \underset{k_2}{\overset{k_{-2}}{\rightleftharpoons}} I \underset{k_1}{\overset{k_{-1}}{\rightleftharpoons}} MC_1 \overset{K_{d_1}}{\leftrightarrow} GAD_o + \text{B-CoA} \quad (3)$$

is crotonyl-CoA, MC_2 is a Michaelis–Menten complex between reduced GAD and crotonyl-CoA, I is the same as in eq 1 and 2, and MC_1, GAD_o, and B-CoA are the same as in eq 1.

The measured value of k_{-1} (from the oxidation reaction) is 0.50 s^{-1}, which is very close to the value estimated for this rate constant from the reduction reaction (0.6 s^{-1}). A lower limit for the value of k_{-2} can be estimated at 220 s^{-1}. The exact value for K_{d_2} cannot be determined from these data. However, from the "dead time" formation of MC_2, K_{d_2} appears to be a rapid equilibrium process. The overall constant ($K_{d_2} \times k_2/k_{-2}$) for the equilibrium between free reduced GAD and intermediate I must be $\sim 10^{-7}$ M or less. This value is estimated from the observation that a 2-fold excess of crotonyl-CoA (20 μM) over reduced GAD (8.1 μM after mixing) resulted in complete formation of the intermediate. Thus, the binding is essentially stoichiometric. For binding to be stoichiometric, the dissociation constant must be ~ 2 orders of magnitude or more below the concentration of the enzyme (8.1 μM, after mixing), i.e., $\sim 10^{-7}$ M in this case. Using this estimate and the estimates for k_{-2} (≥ 220 s^{-1}) and k_2 (0.07 s^{-1}), an upper limit for K_{d_2} of ~ 300 μM can be calculated.

The K_{d_1} step and the involvement of GAD_o in this reaction were inferred from the final (incomplete) extent of reoxidation observed.

We mentioned earlier that our data for the negative substrate dependence of k^s_{app}, in the reduction reaction, did not fit the Kirschner/Halford requirements for a negative dependence of apparent rate on ligand concentration. This becomes evident now that we have an estimate for k_{-2} (220 s^{-1}). A major discrepancy appears when one compares the calculated limiting rate of k^s_{app} at low ligand concentrations for the Kirschner/Halford situation ($k_2 + k_{-2} = 0.07 + 220$ s^{-1}) to the measured rate at low ligand concentration (0.15 s^{-1}). The measured value for k_{-2} is too large to support the Kirschner/Halford requirements.

Binding of Butyryl-CoA to Reduced GAD. Another topic, which was postponed earlier, is the identity of species X in eq 2. By comparison of eq 2 to eq 3, species X could be either MC_2 or GAD_r. The qualitative observations, from the kinetics presented above, are compatible with either species binding butyryl-CoA. However, in order for MC_2 to bind butyryl-CoA, there would need to be two CoA binding sites on GAD, one for crotonyl-CoA and another for butyryl-CoA. No evidence for two such binding sites is available. Therefore, GAD_r is the preferred candidate. We can test whether GAD_r is a suitable candidate for species X by measuring the kinetics of complex formation between butyryl-CoA and reduced GAD. A complex between these two species was inferred by Beinert (Beinert & Page, 1957) from oxidation/reduction studies. If species X is GAD_r, the dissociation rate for the GAD_r·B-CoA complex will be comparable to the measured value for k_{-3} (the dissociation rate from eq 2).

Reduced GAD (15.3 μM) was anaerobically mixed with an equal volume of buffer containing butyryl-CoA. A small, monophasic rise in absorbance was seen at several wavelengths. The maximal absorbance change occurred at ~ 430 nm (see Figure 6). The measured reaction rates were directly dependent on butyryl-CoA concentration and consistent with a second-order reaction. The calculated association rate was

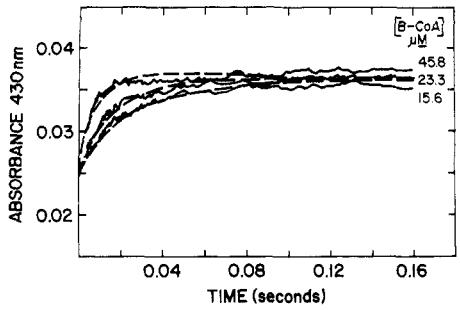

FIGURE 6: Time course for the binding of butyryl-CoA to reduced GAD. Conditions: reduced GAD (15.3 μM) was anaerobically mixed with butyryl-CoA (16.4–91.6 μM) in 50 mM potassium phosphate buffer, pH 7.6 at 4 °C, with a stopped-flow spectrophotometer (2-cm optical path length). The traces shown are for butyryl-CoA concentrations (after mixing) of 15.6, 23.3, and 45.8 μM. The reaction was monitored at 430 nm. The solid lines are the measured time courses. The dashed lines are simulations based on the scheme in eq 4 and the parameters in Tables I and II.

3×10^6 M^{-1} s^{-1}. From the fact that the association was complete in the presence of 15 μM butyryl-CoA, the binding is essentially stoichiometric. We can therefore estimate (as before) a maximum dissociation constant of $\sim 10^{-7}$ M for complex formation. Taking this dissociation constant and the measured association rate, we can calculate an upper limit for the dissociation rate of 0.30 s^{-1}. This rate is close to the value (0.15 s^{-1}) that we estimated for k_{-3} in eq 2. On the basis of these results, we conclude that species X in eq 2 is most reasonably free reduced GAD and k_3 is approximately 3×10^6 M^{-1} s^{-1}.

Binding of Crotonyl-CoA to Oxidized GAD. Earlier steady-state inhibition studies have shown that crotonyl-CoA will bind to oxidized GAD (Hauge, 1956; McKean et al., 1979). From the foregoing discussion, reduction of oxidized GAD by butyryl-CoA or oxidation of reduced GAD by crotonyl-CoA creates an equilibrium that may contain both oxidized GAD and crotonyl-CoA. Since binding of crotonyl-CoA to oxidized GAD is a potential factor in establishing the overall equilibrium end point, we included this reaction in our studies.

When oxidized GAD (13.4 μM) was mixed aerobically with an equal volume of buffer containing crotonyl-CoA, a single, first-order reaction was observed (Figure 7, panel A). The measured rate was linearly dependent on the concentration of crotonyl-CoA (Figure 7, panel B). Analysis of Figure 7, panel B, gives an association rate of 9.8×10^5 M^{-1} s^{-1} (k_{-4}) and a dissociation rate of 20 s^{-1} (k_4). An equilibrium dissociation constant of 20 μM can be calculated from these measured rates.

Crotonyl-CoA perturbs the spectrum of oxidized GAD, shifting the 446-nm peak to 454 nm and reducing the peak extinction coefficient to 14.8 mM^{-1} cm^{-1} while shifting the 372-nm peak to 379 nm and reducing the peak extinction coefficient to 10.5 mM^{-1} cm^{-1}. A difference spectrum (Δ absorbance, crotonyl-CoA complexed GAD minus uncomplexed GAD) is shown in Figure 8. Spectra were taken at the end of the kinetic reaction, in the stopped-flow spectrophotometer. The absorbance difference between the peak at 490 nm and the valley at 440 nm (a $\Delta\Delta$ absorbance) is plotted versus the concentration of crotonyl-CoA in the inset to Figure 8. A theoretical line for a dissociation constant of 12 μM and a total Δ absorbance change of 0.054 ($\Delta\Delta$ extinction change of 4.0 mM^{-1} cm^{-1}) can be fit to the data. This equilibrium dissociation constant is in reasonable agreement with the dissociation constant taken from the kinetic data (20 μM). Both values are in reasonable agreement with the previously reported inhibition constant (15 μM) for crotonyl-CoA binding

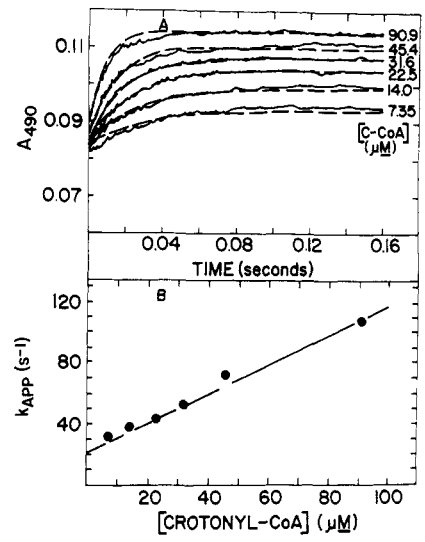

FIGURE 7: Time course for the binding of crotonyl-CoA to oxidized GAD. Conditions: oxidized GAD (13 μM) was aerobically mixed with crotonyl-CoA (15–182 μM) in 50 mM potassium phosphate buffer, pH 7.6 at 4 °C, with a stopped-flow spectrophotometer (2-cm optical path length). Panel A: The solid lines are the measured time courses. The dashed lines are simulations based on the scheme in eq 4 and the parameters in Tables I and II. The after mixing crotonyl-CoA (C-CoA) concentrations are listed in the margin. The reaction was monitored at 490 nm. Panel B: A plot of the apparent rate versus the crotonyl-CoA concentration.

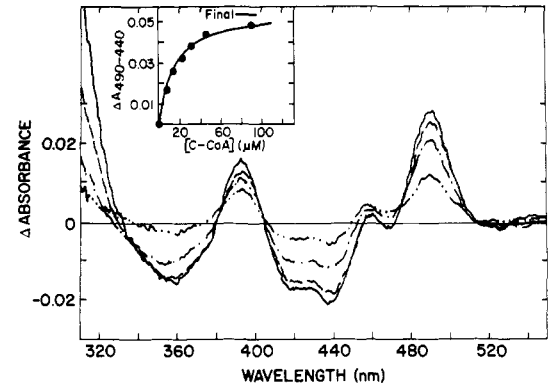

FIGURE 8: Difference spectra from the reaction of oxidized GAD with crotonyl-CoA. Conditions: same as in Figure 7. Difference spectra (complex minus oxidized GAD) are shown for complexes involving crotonyl-CoA concentrations (after mixing): 7 μM (dash-dot-dot line); 25 μM (dash-dot line); 50 μM (dashed line); 100 μM (solid line). All spectra were recorded in the stopped-flow spectrophotometer immediately after the kinetic changes had finished. Some of the spectra have been omitted for clarity. Inset: The absorbance difference between the valley at 440 nm and the peak at 490 nm taken from the Δ absorbance data plotted versus the concentration of crotonyl-CoA. The solid line is a theoretical curve calculated for a single binding event with a dissociation constant of 12 μM and a total Δ absorbance of 0.054. The end point for this titration curve is marked "Final".

to oxidized GAD (Hauge, 1956).

Simulation. We have now described the events involved in the reduction of GAD by butyryl-CoA in sufficient detail to draw an overall mechanism for the reaction. Combining eq 1–3 with the oxidized GAD/crotonyl-CoA binding reaction, we obtain the mechanism shown in eq 4. MC_1 is a Mi-

$$\begin{array}{ccccccccc} & \mathrm{GAD_o \cdot C\text{-}CoA} & & & & & & \mathrm{GAD_r \cdot B\text{-}CoA} & \\ \mathrm{C\text{-}CoA}\ k_{-4}\big\uparrow\big\downarrow k_4 & & & & & & & \mathrm{B\text{-}CoA}\ k_3\big\uparrow\big\downarrow k_{-3} & \\ \mathrm{GAD_o} + \mathrm{B\text{-}CoA} & \xrightarrow{K_{d_1}} & \mathrm{MC_1} & \underset{k_{-1}}{\overset{k_1}{\rightleftharpoons}} & \mathrm{I} & \underset{k_{-2}}{\overset{k_2}{\rightleftharpoons}} & \mathrm{MC_2} & \xrightarrow{K_{d_2}} & \mathrm{C\text{-}CoA} + \mathrm{GAD_r} \end{array} \qquad (4)$$

Table I: Rate and Equilibrium Constants for the Steps in the Reaction of GAD with Butyryl-CoA

parameter	measured value	best fit to simulation value
	Proteobutyryl-CoA	
k_1 (s^{-1})	1.7	1.9
k_{-1} (s^{-1})	0.6	0.45
k_2 (s^{-1})	0.07	0.07
k_{-2} (s^{-1})	220	450
k_3 ($M\ s^{-1}$)	3×10^6	3×10^6
k_{-3} (s^{-1})	0.15	0.20
k_4 (s^{-1})	20	16
k_{-4} ($M\ s^{-1}$)	9.8×10^5	1.2×10^6
K_{d_1} (μM)	37	80
K_{d_2} (μM)	300[a]	20
	α,β-Dideuteriobutyryl-CoA	
k^*_1 (s^{-1})		0.127
k^*_{-1} (s^{-1})		0.033

[a] Upper limit value.

chaelis–Menten complex of oxidized GAD and butyryl-CoA, I is a charge-transfer complex of reduced GAD and crotonyl-CoA, and MC_2 is a Michaelis–Menten complex of reduced GAD and crotonyl-CoA. The rate and equilibrium constants have all been estimated and are summarized in Table I. This model predicts the release of crotonyl-CoA during the establishment of equilibrium. The amount of crotonyl-CoA released will increase as the butyryl-CoA concentration is increased, since formation of GAD_r·B-CoA will be increased. Consistent with this prediction, we detected the presence of crotonyl-CoA in the medium after completion of the fast phases. The amount of free crotonyl-CoA varied from 24% of the starting GAD concentration, in the presence of 88 μM butyryl-CoA, to 41% of the starting GAD concentration, in the presence of 410 μM butyryl-CoA.

This mechanism was used to simulate all of the rate data shown in Figures 2, 4, 6, and 7. Simulation of eq 4 was accomplished numerically. The differential equations describing the formation and decay of each species were written by inspection of eq 4. This differential equation set was then solved by using a fourth-order Runge–Kutta numerical method (Forsythe et al., 1977). The resultant concentration versus time array for each species was multiplied by the appropriate extinction coefficient, and the total absorbance at each time point was calculated by summing the contributions from each species. Initial estimates for kinetic parameters and extinction coefficients were taken from Tables I and II. "Goodness of fit" of the absorbance versus time trace was determined by visual comparison of the data to the simulation. Kinetic parameters and/or extinction coefficients were changed manually and the numerical solution was repeated. Adjustments were made in a trial-and-error fashion. Best fit was declared when visual inspection indicated that all 23 simulation traces matched the data traces. Mathematically rigorous fitting regimes were precluded from this effort due to the fact that comparing 23 traces, from 4 different reactions, at 2 different wavelengths over several different time ranges exceeded the capacity of our computer resources. The best fit lines are overlaid on each data trace in every figure. The final set of best fit parameters are shown in Tables I and II. The close correspondence between the measured and simulated rate traces provides strong evidence for the suitability of the mechanism in eq 4. This mechanism is very similar to that originally proposed for this reaction by Beinert (Beinert & Page, 1957) on the basis of ligand binding and oxidation/reduction studies.

It is interesting to note that for butyryl-CoA concentrations below 100 μM this mechanism predicts that the dominant species at equilibrium will be the reduced enzyme/crotonyl-CoA charge-transfer intermediate I. This form of the enzyme has been previously shown to be the species that reacts with the natural electron acceptor for GAD, electron-transferring flavoprotein (Hall et al., 1979; Gorelick et al., 1985).

Reduction of Oxidized GAD with Deuteriated Butyryl-CoA. Unusually large deuterium isotope effects are observed in both apparent rates when oxidized GAD is reduced by perdeuterated butyryl-CoA (Reinsch et al., 1980; Pohl et al., 1986). The large value for the isotope effect has been shown to be due to the transfer of two protons/deuterons from butyryl-CoA to oxidized GAD during the transition state (Pohl et al., 1986). However, there still remains the puzzling fact that rates for both formation and decay of the charge-transfer intermediate (I) exhibit isotope effects. Formation of I involves reduction of the flavin and, as such, would be expected to have a deuterium isotope effect. However, if eq 4 is correct, the decay of I is limited by steps involving no obvious proton/deuteron transfer and should therefore not be sensitive to deuteriation of butyryl-CoA.

This dilemma stems from the manner in which the isotope data were analyzed. Previous workers measured the apparent reduction rates (k^f_{app} and k^s_{app}) with deuteriated and nondeuteriated substrates. They then compared slow phase to slow phase and fast phase to fast phase in each reaction to determine the isotope effect. Isotope effects are, however, directly related to intrinsic rate constants and only indirectly related to the measured, apparent rate constants. This is especially significant for multistep, reversible reactions in which the intrinsic rate constants for the rate-limiting steps are all of similar magnitude. For the GAD/butyryl-CoA reaction described in eq 4, each apparent rate (k^f_{app} and k^s_{app}) represents a complex combination of the limiting intrinsic rate constants (k_1, k_{-1}, k_2, and k_{-3}). An isotope effect in the intrinsic rate constants k_1 and k_{-1} can be reflected in both apparent rates. This argument is developed more thoroughly in the Appendix, part B. In essence, however, it is possible to reproduce the isotope effect data by using eq 4 and decreasing the rates of k_1 and k_{-1} only. This is illustrated in Figure 9.

Table II: Extinction Coefficients for the Components of the Reaction of GAD with Butyryl-CoA

	extinction coefficients ($mM^{-1}\ cm^{-1}$)							
	measured				best fit to simulation			
component	430 nm	450 nm	490 nm	560 nm	430 nm	450 nm	490 nm	560 nm
GAD_o	*a*	15.4	6.25	0	*a*	15.2	6.25	0
MC_1	*a*	NM[b]	*a*	0	*a*	13.9	*a*	0
I	*a*	4.1	*a*	2.8	*a*	4.8	*a*	2.9
MC_2	*a*	NM[b]	*a*	0	*a*	4.8	*a*	0
GAD_r	1.6	1.5	*a*	0	1.6	1.5	*a*	0
GAD_o·C-CoA	*a*	14.9	8.65	0	*a*	14.8	8.90	0
GAD_r·B-CoA	NM[b]	NM[b]	*a*	0	2.4	5.0	*a*	0

[a] Values that were not applicable to the calculations. [b] Not measured.

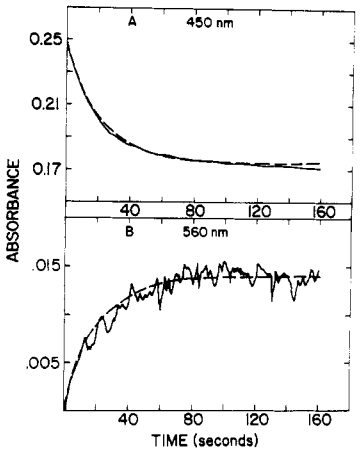

FIGURE 9: Reduction of oxidized GAD by α,β-dideuteriobutyryl-CoA. Conditions: same as in Figure 2 except that α,β-dideuteriobutyryl-CoA (35 μM) was used in place of butyryl-CoA. Panel A: Time course of the reaction at 450 nm over 160 s. Panel B: Average of three time course traces at 560 nm over 160 s. The solid lines are the measured time courses. The dashed lines are simulations based on the scheme in eq 4 and the parameters in Tables I and II.

When oxidized GAD (16.4 μM) was mixed anaerobically with an equal volume of buffer containing α,β-dideuteriobutyryl-CoA (70 μM), a single first-order reaction was observed (in the first 3 min). There was a loss of absorbance at 450 nm and a small rise at 560 nm. The measured rate (0.05 s^{-1}) was slower than either the apparent formation (k^f_{app} = 1.7 s^{-1}) or apparent decay (k^s_{app} = 0.15 s^{-1}) rates for I, measured using proteobutyryl-CoA under comparable conditions. The rate traces could nonetheless be fit to eq 4, using the rate constants and extinction coefficients in Tables I and II, if the values of k_1 and k_{-1} were both reduced by a factor of 15. No other changes were required. We chose to place the same isotope effect on both the foward and reverse rates for this step, since earlier work had indicated an equilibrium isotope effect for GAD of $\sim$1 (Pohl et al., 1986).

Supplementary Data at 25 °C. Reduction of oxidized GAD with butyryl-CoA and oxidation of reduced GAD with crotonyl-CoA were also examined at 25 °C. Though this data set was less extensive, the time course traces, at both 450 and 560 nm, could all be fit to the model in eq 4, using a single set of rate constants and extinction coefficients (data not shown). The effect of using α,β-dideuteriobutyryl-CoA as substrate could also be fit to eq 4. Unlike the 4 °C case, in the presence of α,β-dideuteriobutyryl-CoA the traces were distinctly biphasic. Both phases exhibited markedly reduced apparent rates, a 19-fold reduction for the fast phase and a 9.4-fold reduction for the slow. The measured rates (with both p; oteo- and dideuteriobutyryl-CoA) were comparable to those reported by Pohl et al. (1986). Nevertheless, both phases could be accurately fit to eq 4 by reducing the value of only k_1 and k_{-1}. In this case, both rates were reduced by a factor of 25.

Discussion

We have described the rapid reaction kinetics for the reactions (1) oxidized GAD/butyryl-CoA, (2) oxidized GAD/crotonyl-CoA, (3) reduced GAD/crotonyl-CoA, and (4) reduced GAD/butyryl-CoA. From the data, we constructed the mechanism in eq 4. The various enzyme forms in the mechanism were directly implicated from a qualitative appraisal of the data. Most species had been proposed previously: GAD_o·C-CoA, on the basis of steady-state product inhibition (Hauge, 1956); GAD_r·B-CoA, on the basis of inhibition of oxidation by propionyl-CoA (Beinert & Page, 1957); MC_1, on the basis of steady-state kinetics (Hauge, 1956; Hall & Kamin, 1975; McKean et al., 1979); and I, on the basis of substrate reduction studies (Beinert & Page, 1957; Thorpe et al., 1979; Hall et al., 1979; Reinsch et al., 1980; Ikeda et al., 1985c; Pohl et al., 1986). The identity of the various species is generally agreed upon, except for intermediate I. We have assigned I to be a charge-transfer species between reduced GAD and crotonyl-CoA. This is based on the spectrum of I (Figure 5, open circles), which shows the flavin chromophore to be reduced, in conjunction with a long-wavelength absorbance band. Our assignment is in accord with a substantial amount of evidence, which has been documented in the introduction. We will return to the question of the structure of intermediate I later in the discussion.

We used the mechanism in eq 4 to simulate all of the data from all four reactions, using a single set of kinetic and extinction parameters. The close correspondence between data and simulation for the 23 time course traces (both the rapid and slow phases) makes us confident that the proposed mechanism accurately describes the interaction of GAD with butyryl-CoA and crotonyl-CoA. This mechanism for GAD is not new; Beinert and co-workers (Hauge, 1956; Beinert & Page, 1957; Steyn-Parvé & Beinert, 1958) developed a similar mechanism on the basis of equilibrium binding, steady-state, and oxidation/reduction studies. The steps leading to intermediate I have been independently proposed by several groups (Thorpe et al., 1979, 1981; Pohl et al., 1986; McKean et al., 1979). We have reaffirmed and refined the mechanism, added rate and equilibrium constants, and made the model more useful for purposes of discussing the behavior of GAD.

An important feature of eq 4 is the manner in which butyryl-CoA and crotonyl-CoA compete for reduced GAD. Both equilibria strongly favor complexation. Therefore, under no conditions will free GAD_r be present in significant concentration. The overall dissociation equilibrium constant between I and GAD_r is $K_{d_2} \times k_2/k_{-2} = 3 \times 10^{-9}$ M (using best fit values), while that between GAD_r·B-CoA and GAD_r is $k_{-3}/k_3 = 7 \times 10^{-8}$ M. Thus, crotonyl-CoA is approximately 25-fold more effective at binding GAD_r than is butyryl-CoA. However, in a single turnover, reductive experiment, the concentration of free crotonyl-CoA cannot be greater than the concentration of the enzyme. But the levels of butyryl-CoA can be increased at the discretion of the experimenter. At sufficiently high concentration, butyryl-CoA will force all of the enzyme into the GAD_r·B-CoA complex. Thus, we can rationalize the rate traces in Figure 2. Partial formation of intermediate I, in the first 3 s, causes a loss in absorbance at 450 nm and a rise in absorbance at 560 nm. The level of intermediate I is then partially reduced by virtue of the formation of an equilibrium amount of GAD_r·B-CoA, in the second phase. The loss of I induces a reequilibration and further loss in the residual GAD_o/MC_1 forms. GAD_r·B-CoA has spectral properties similar to those of the GAD_r·C-CoA Michaelis–Menten complex (MC_2) seen in Figure 5 (closed squares). Thus, in the second phase, the absorbance at 450 nm decreases due to the shift of oxidized GAD forms to I and absorbance at 560 nm decreases due to a shift of I to GAD_r·B-CoA.

Formation of GAD_r·B-CoA provides the thermodynamic driving force for the decay of intermediate I. Were the dissociation constant (k_{-3}/k_3) between GAD_r and GAD_r·B-CoA larger, butyryl-CoA would be a less effective competitor against crotonyl-CoA and larger amounts of intermediate I would be seen.

The tendency to form the GAD_r·acyl-CoA complex with consequent loss of 560-nm absorbance in the course of re-

duction is most pronounced with butyryl-CoA as reductant. However, loss of 560-nm absorbance at elevated octanoyl-CoA concentrations has been noted by Thorpe et al. (1979) and can be seen in the data of Ikeda et al. (1985c). This indicates that the phenomenon occurs with octanoyl-CoA as well.

The acyl-CoA/enoyl-CoA competition for reduced GAD is not the only factor in eq 4 that affects the level of intermediate I. The formation steps, K_{d_1} and k_1/k_{-1}, determine the affinity of oxidized GAD for the acyl-CoA. Having two steps in the process leading to I increases the potential complexity in the mechanism. If the k_1/k_{-1} step favors the formation of I for a particular acyl-CoA, then MC_1 will not be a prominent feature and a titration of oxidized GAD by that acyl-CoA will have the appearance of a reduction. If, on the other hand, the k_1/k_{-1} step is unfavorable for the formation of I, then MC_1 will dominate and a titration of oxidized GAD by such an acyl-CoA will have the appearance of a ligand binding perturbation on the oxidized enzyme.

The amount of I at equilibrium can thus be controlled by both the relative affinity of the acyl-CoA/enoyl-CoA couple for reduced GAD and the k_1/k_{-1} equilibrium. This affords a straightforward rationale for the variable amounts of I observed when oxidized GAD is reacted with acyl-CoA substrates of various chain length.

We can illustrate these principles by comparing the behavior of the reductants butyryl-CoA (short chain), octanoyl-CoA (medium chain), and palmitoyl-CoA (long chain). Data for this comparison can be found in the work of Ikeda et al. (1985c), Thorpe et al. (1979), or Hall et al. (1979). Titrations with these three substrates indicate that palmitoyl-CoA and octanoyl-CoA bind very tightly to oxidized GAD, while butyryl-CoA has a measurable dissociation constant of $\sim 30\ \mu M$. The spectra of the complexes resulting for each of these titrations are unique.

Addition of octanoyl-CoA to oxidized GAD results in marked loss of absorbance in the 450-nm region and the appearance of substantial long-wavelength absorbance. The end point of a titration closely resembles the spectrum of intermediate I in Figure 5 (open circles). Such behavior is consistent with a low dissociation constant for K_{d_1} and a large k_1/k_{-1} ratio. This would result in direct conversion of GAD_o to I. Tight, stoichiometric binding of octanoyl-CoA also means that in a titration of GAD effectively no free octanoyl-CoA is available to compete with octenoyl-CoA for GAD_r. Thus, shifting of the overall equilibrium toward GAD_r·octanoyl-CoA would be minimized. The net result appears to be optimum formation of intermediate I.

Palmitoyl-CoA also binds tightly to oxidized GAD. But in this case much less bleaching occurs, the 446-nm absorbance maximum is shifted toward the red, and very little long-wavelength absorbance appears. These changes are indicative of a ligand binding perturbation on the spectrum of oxidized enzyme. Such behavior would be consistent with a very low dissociation constant K_{d_1} and a k_1/k_{-1} ratio considerably less than 1. This would result in formation of MC_1 with minimal conversion to intermediate I. The low levels of free palmitoyl-CoA in titration experiments, together with effectively no reduction of GAD, would combine to make acyl-CoA/Enoyl-CoA competition for GAD_r an insignificant factor in establishing this equilibrium.

Butyryl-CoA causes extensive bleaching of the 446-nm chromophore, as we have demonstrated in Figures 2 and 3. However, concentrations of butyryl-CoA approaching the millimolar level are required. Furthermore, for any given level of reduction at 446 nm, the amplitude of the 560-nm band is decidedly less with butyryl-CoA than it is with octanoyl-CoA. Such behavior is consistent with a higher value for the dissociation constant K_{d_1} than is found for palmitoyl-CoA or octanoyl-CoA and a k_1/k_{-1} ratio greater than 1. This would require higher levels of butyryl-CoA to saturate GAD_o but no significant buildup of MC_1. The transient appearance of MC_1 has been noted when perdeuteriobutyryl-CoA is used as substrate (Pohl et al., 1986). In addition, the elevated levels of free butyryl-CoA are sufficient to promote competition with crotonyl-CoA for GAD_r. This would deplete intermediate I to form GAD_r·butyryl-CoA. Thus, optimal levels of I would never be attained, and maximal formation of the long-wavelength band would not be seen.

Thus, eq 4 adequately accounts for the differences in behavior observed when butyryl-CoA, octanoyl-CoA, and palmitoyl-CoA are used as substrates. There is no necessity for invoking unprecedented schemes such as that proposed by Ikeda et al. (1985c), which require that "although flavin bleaching is observed, this does not represent the chemical reduction or redox state of the enzyme-bound FAD". The suggestion that flavin bleaching is not associated with chemical reduction of the FAD is also inconsistent with the fact that the rate of flavin bleaching shows isotope effects with α- and β-deuteriated substrates (Pohl et al., 1986).

On the basis of the above considerations, one would predict that altering the k_1/k_{-1} equilibrium would affect the overall affinity of an acyl-CoA substrate for oxidized GAD as well as the discrimination between MC_1 and I. The k_1/k_{-1} equilibrium can be changed by substituting flavins of different redox potential into GAD. When 8-Cl-FAD GAD is reacted with either butyryl-CoA or palmitoyl-CoA, formation of intermediate I is nearly stoichiometric (Thorpe & Massey, 1983). 8-Cl-FAD has a more positive redox potential than native FAD and as such is more readily reduced. Thus, the k_1/k_{-1} equilibrium is increased. This will lower the overall dissociation constant between GAD_o and I. For the loosely associated butyryl-CoA, this will result in tighter binding and increased formation of I. For the tight-binding palmitoyl-CoA, increasing the k_1/k_{-1} ratio will enhance the formation of I at the expense of MC_1.

The above discussion outlines the operational features of eq 4. For either short-chain (butyryl-CoA) or long-chain (palmitoyl-CoA) reductants, the equilibrium concentration of intermediate I is low. The low levels of I arise from different aspects of the mechanism, but in both cases, the net effect results in a poor substrate. For medium chain (octanoyl-CoA), GAD stabilizes intermediate I. Stabilization of I is correlated with an increase in the steady-state rate of electron transfer (Hauge, 1956; Beinert & Page, 1957; Ikeda et al., 1985c). This is consistent with the observation that intermediate I is the preferred reactant for the physiological electron acceptor, electron-transferring flavoprotein (Hall & Lambeth, 1980; Gorelick et al., 1985). Thus, eq 4 can satisfactorily rationalize the steps in the functioning of GAD.

The issue of half-site reactivity for butyryl-CoA has been raised by McKean et al. (1979). These workers have shown that acetoacetyl-CoA binds to oxidized GAD in a ratio of 2 ligands/tetrameric GAD. They combined this observation with the finding that butyryl-CoA bleached the flavin chromophore by 62% (40–60% bleaching is frequently reported) to suggest that butyryl-CoA may also react with only half of the flavin sites. We do not agree with the proposal for half-site reactivity with butyryl-CoA for the following reasons. Use of the extent of bleaching as a measure of the extent of reduction implicitly assumes that complete reduction requires

100% bleaching. Dithionite reduction, in fact, leads to only 90% bleaching at 446 nm (Figure 5, dotted line), while substrate reduction produces yet less bleaching, even with optimal substrates such as octanoyl-CoA (Beinert & Page, 1957; Thorpe et al., 1979; Hall et al., 1979; Ikeda et al., 1985c; Auer & Frerman, 1980). This and the following observations suggest that the end point for the reduced enzyme/product complex may retain significant absorbance at 446 nm. Supporting observations include (1) the final spectrum at the end of the slow phase, shown in Figure 1, (2) the fully formed spectrum of the long-wavelength intermediate obtained by reacting crotonyl-CoA with reduced GAD, shown in Figure 5, open circles, (3) the spectral perturbations that appear on binding either crotonyl-CoA (Figure 5, closed squares) or butyryl-CoA (Figure 6) to reduced GAD, and (4) literature precedents for ligand-induced perturbations of reduced flavoenzyme spectra, which include (a) *p*-hydroxybenzoate with *p*-hydroxybenzoate hydroxylase (Entsch et al., 1976), (b) piperidine-2-carboxylate or pyruvate/NH_4^+ with D-amino acid oxidase (Massey & Ghisla, 1974), and (c) 2-hydroxyphenyl propionate plus 3-acetylpyridine–NAD with melilotate hydroxylase (Schopfer & Massey, 1979). On the basis of these considerations, it seems reasonable to suggest that the proper end point for the substrate reduction should be equivalent to the spectrum of intermediate I (Figure 5, open circles). With intermediate I as the end point, 89% reduction occurs in the fast phases when 845 μM butyryl-CoA is used. This is inconsistent with half-site reactivity for butyryl-CoA. Half-site reactivity is also inconsistent with the reaction of oxidized GAD with 3,4-pentadienoyl-CoA. This substrate analogue reduces GAD and forms an irreversible, covalent adduct with the reduced flavin in a strictly monophasic process involving all of the flavin (Wenz et al., 1985).

We have already discussed how eq 4 can account for the unusual negative substrate dependence seen for k^s_{app} (Reinsch et al., 1980; Pohl et al., 1986). We have also described how eq 4 can account for the observation of large deuterium isotope effects in both k^f_{app} and k^s_{app} (Reinsch et al., 1980; Pohl et al., 1986). We will now address the issue of the structure of intermediate I.

Using rat liver mitochondrial GAD, Tanaka and co-workers have recently described a series of deuterium-exchange experiments (Ikeda et al., 1985b) from which they concluded that frank reduction of the flavin by octanoyl-CoA does not occur unless an electron acceptor is included in the reaction. They proposed that in the absence of an electron acceptor GAD abstracts the C-2 proton from the substrate to form a carbanion. Then "the carbanion and oxidized flavin form a resonance hybrid in which the incipient hydride ion at C-3 of the carbanion mediates the resonance structure". Adding an electron acceptor, such as electron-transferring flavoprotein, "abstracts electrons from the alloxazine of the enzyme-bound flavin ... completing the flow of electrons from substrate via enzyme-FAD, with a transfer of hydride ion to N-5 of alloxazine". Thus, intermediate I in eq 4 would be a resonance hybrid of oxidized FAD and the carbanion of butyryl-CoA. This is quite different from the interpretation of intermediate I as a charge-transfer complex between reduced GAD and enoyl-CoA.

These workers based their interpretation on two observations. First, they found that denaturing a reaction mixture containing a substantial fraction of intermediate I with 0.1 M KOH did not release the enoyl-CoA product as had been expected (Ikeda et al., 1985b). This experiment assumed that all forms of GAD denature at the same rate. This assumption is incorrect. Oxidized GAD is more sensitive to denaturation than is the reduced form (Madden et al., 1984). Since the reaction mixture is in equilibrium, as described in eq 4, denaturating the mixture will result in (1) the oxidized GAD being eliminated first, (2) a shift of the equilibrium toward oxidized GAD; and (3) reduction of the enoyl-CoA back to the acyl-CoA by the reduced GAD. Hence, no free enoyl-CoA would be expected.

Second, Tanaka and co-workers found that incubating octanoyl-CoA with GAD in D_2O, in the absence of an electron acceptor, resulted in exchange of only the C-2 proton (on octanoyl-CoA) for deuterium. The C-3 proton, which was released from octanoyl-CoA (along with the C-2 proton) during oxidation, was not exchanged (Ikeda et al., 1985b). It was assumed that "if a C-3 hydrogen of the substrate had been transferred to N-5 of isoalloxazine, then deuterium should have been incorporated into the C-3 of the substrate, because the N-5 proton of FAD is known to rapidly exchange with water protons". However, intermediate I is an enzyme/ligand complex. Early work indicated that the flavin of GAD was protected from contact with solvent-borne reagents (molecular oxygen and dithionite) by the presence of substrates/products (Beinert & Page, 1957; Steyn-Parvé & Beinert, 1958). Therefore, there is no reason to assume that a proton on N-5 would necessarily be exchanged with solvent, as long as intermediate I remains stable. As we have discussed, in the presence of octanoyl-CoA, the mechanism of GAD is engineered to stabilize intermediate I. Thus, it can be argued that the reaction of octanoyl-CoA with oxidized GAD leads to a reduced GAD/octenoyl-CoA complex (intermediate I) wherein the proton on N-5 of the isoalloxazine is protected from solvent. Dissociation of the complex to free reduced GAD and octenoyl-CoA is unfavorable. We are left with a reaction that is effectively blocked at the level of the reduced enzyme/product complex. Reversal of the reduction reaction, by the principles of microscopic reversibility, would result in the transfer of the proton from the N-5 of isoalloxazine back to the C-3 of octanoyl-CoA. An active equilibrium between oxidized GAD and intermediate I under these conditions could account for the observed selective exchange of the C-2 proton without invoking a resonance hybrid intermediate. An active equilibrium can be inferred from the rates of eq 4 and has been demonstrated by substrate displacement experiments (Steyn-Parvé & Beinert, 1958).

A further difficulty with the model of Tanaka and coworkers stems from the requirement that the C-2 proton be removed from octanoyl-CoA without removing the C-3 proton. This requirement is contrary to the results from experiments using deuteriated butyryl-CoA to reduce GAD. These experiments have shown that both protons are involved, in a concerted manner, in the reduction step (Pohl et al., 1986). Separation of the proton abstraction process (C-2) from the reduction of the flavin (C-3) when using octanoyl-CoA is therefore unlikely.

At this point, we would like to comment on some differences between the present work and a previous study by Pohl et al. (1986). That study also dealt with the kinetics of GAD, focusing on the substrate isotope effects. In the present study, smaller isotope effects, tighter binding of CoA derivatives, and a difference in the value of equilibrium between MC_1 and I were found. These differences are reasonably attributed to the different temperatures (25 versus 4°C) at which the two sets of experiments were conducted. The essence of the previous work, (1) the finding of large isotope effects on the rate of formation of I when using α- and β-deuteriated substrates

and (2) the multiplicative nature of these isotope effects, is fully supported by the present study. Details of the kinetic analysis in that work were hampered by an incomplete appreciation of the overall GAD mechanism.

Appendix[2]

(A) We have found that the mechanism described in eq 5 exhibits an unexpected versatility with regard to the effect of substrate concentration on the apparent reaction rate. It is

$$A \underset{k_{-1}}{\overset{k_1}{\rightleftharpoons}} B \underset{k_{-2}}{\overset{S,k_2}{\rightleftharpoons}} C \qquad (5)$$

$$A \underset{k_{-1}}{\overset{S,k_1}{\rightleftharpoons}} B \underset{k_{-2}}{\overset{k_2}{\rightleftharpoons}} C \qquad (6)$$

possible to define situations in which the apparent rate either increases, decreases, or remains unchanged (excluding saturation) as the substrate concentration increases. The mechanism in eq 6, though quite similar to eq 5, describes a situation in which the apparent rate always increases as the substrate concentration increases (until saturation is reached). This difference between eq 5 and 6 is not generally appreciated since eq 6 is commonly discussed in theoretical treatments of rapid reaction, enzyme kinetics, while eq 5 is generally not considered. In eq 5, A and B are uncomplexed enzyme forms, S is the ligand, and C is the enzyme/ligand complex. In eq 6, A is uncomplexed enzyme, S is the ligand, and B and C are different enzyme/ligand complexes (C could be an enzyme/product form). An appreciation of the flexibility inherent in eq 5 can be gained by evaluating the apparent rate (k_{app}) by the steady-state approximation procedure (Strickland et al., 1975). The differential equations that describe the time course of eq 5 are

$$d[A]/dt = k_{-1}[B] - k_1[A]$$

$$d[B]/dt = k_1[A] + k_{-2}[C] - k_{-1}[B] - k_2[B][S]$$

$$d[C]/dt = k_2[B][S] - k_{-2}[C]$$

Setting $d[B]/dt$ equal to zero (the steady-state assumption) and solving these equations for A yields

$$[A] = \text{const}(1 - e^{-k_{app}t})$$

where

$$k_{app} = \frac{k_{-1}k_{-2} + k_1k_2[S] + k_1k_{-2}}{k_{-1} + k_2S + k_{-2}}$$

As $k_2[S] \rightarrow$ infinity, $k_{app} \rightarrow k^h_{app} \rightarrow k_1$ (the limiting rate at high concentration of S). This result is independent of the values for the other rate constants. As $k_2[S] \rightarrow 0$, $k_{app} \rightarrow k^l_{app} \rightarrow [(k_1 + k_{-1})k_{-2}/(k_{-1} + k_{-2})]$ (the limiting rate at low concentration of S).

This lower limit expression can be simplified by making some limiting case assumptions: if $k_{-2} \gg k_{-1}$ (Kirschner/Halford condition), then $k^l_{app} \rightarrow k_1 + k_{-1}$.

This is the condition employed by Kirschner et al. (1966) and Halford (1972). It predicts that the apparent rate at low concentration of S, $k^l_{app} = k_1 + k_{-1}$, will be greater than the apparent rate at high concentration of S, $k^h_{app} = k_1$.

In an alternate limiting case assumption, if $k_{-1} \gg k_1$ and k_{-2} (general condition), then $k^l_{app} \rightarrow k_{-2}$.

This condition poses a situation in which increasing the substrate concentration will cause the apparent rate to (1) decrease if $k_1 < k_{-2}$, (2) increase if $k_1 > k_{-2}$, or (3) remain unchanged if $k_1 = k_{-2}$. Since there is no a priori reason for fixing the relative values of k_1 and k_{-2} in any particular order, all three possibilities are viable. The first situation covers the circumstances of k^s_{app} in our current study of GAD. The second situation provides eq 5 with the substrate/reaction rate profile commonly expected for rapid reaction kinetics. The third situation presents itself as a reaction that increases in extent as the substrate concentration increases but does not change in rate. An example of this situation was found earlier in a study on melilotate hydroxylase (Schopfer & Massey, 1979).

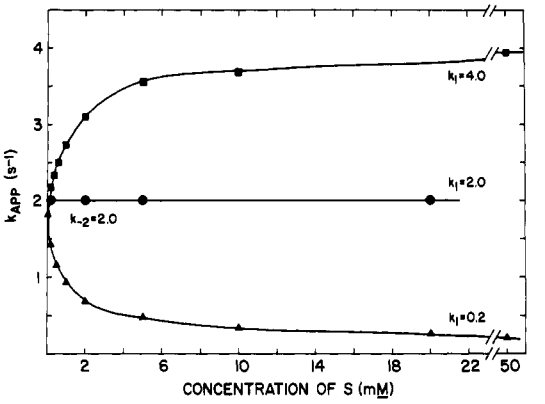

FIGURE 10: Plots of apparent rate versus ligand concentration for simulations of the mechanism in eq 5. Conditions: The starting concentration of A was 10 μM. Rate constants were k_1 = 0.2 (triangles), 2.0 (circles), or 4.0 (squares) s^{-1}, k_{-1} = 2.0 s^{-1}, $k_2 = 2 \times 10^3$ M^{-1} s^{-1}, and k_{-2} = 2.0 s^{-1}. The concentration of S was varied from 0.05 to 100 mM (some points are omitted for clarity). The formation of C was monitored. The apparent rate (k_{app}) of the slow phase, i.e., after a steady state was established, was measured. A small fast phase sometimes was seen.

In practice, this "general pattern" of substrate dependence is retained even when k_{-1} is of the same magnitude as k_1 and k_{-2}. This is illustrated in Figure 10, where eq 5 is simulated, using a fourth-order Runge–Kutta method. On the basis of a large number of simulations made for eq 5, using a wide range of rate constants, it can be stated as a general property that the limiting rate at low substrate concentration (k^l_{app}) varies smoothly from $k_1 + k_{-1}$ (when $k_{-1} \ll k_{-2}$) to k_{-2} (when $k_{-1} \gg k_{-2}$). The exact value for k^l_{app} is difficult to predict when the values for k_1, k_{-1}, and k_{-2} all are of the same magnitude. The limiting rate at high substrate concentration (k^h_{app}) is always k_1.

In the treatment of eq 5 by the steady-state procedure, it is understood that conditions in which k_1, k_{-1}, and k_{-2} approach the same order of magnitude violate the steady-state assumptions. However, the predictions made from the steady-state equation have been qualitatively verified by simulating eq 5 under conditions ranging from those that are compatible with the steady-state assumption to those that are not. The steady-state treatment is remarkable in that it provides a qualitatively accurate picture of the progress of events well outside the limits for which it is quantitatively well-defined.

Species A was used in the steady-state solution for eq 5 in order to obtain an expression for k_{app} that would predict the substrate dependence observed in practice. Solving eq 5 for species C yields an expression for k_{app} that does not predict the Kirschner/Halford situation. A comparable dilemma exists when the steady-state solution is applied to eq 6. Different expressions for k_{app} are obtained depending on whether one solves for species A or C. In that case, the solution obtained by solving for species C is the most applicable (Strickland et al., 1975).

The reaction described in eq 5 is commonly considered to start with species A and B already equilibrated. This leads

[2] Appendix by L.M.S.

Table III: Rate Constants and Measured Rates from Simulations on the Effect of Deuterium Isotopes on the Kinetics of Reversible Mechanisms[a]

$$A \underset{k_{-1}}{\overset{k_1}{\rightleftharpoons}} B \underset{k_{-2}}{\overset{k_2}{\rightleftharpoons}} C$$

k_H/k_D	k_1	k_{-1}	k_2	k_{-2}	k^f_{app}	app isotope effect[b]	k^s_{app}	app isotope effect[b]
1	2.0	0.5	0.2	0.2	2.50	1.00	0.343	1.00
2	1.0	0.25	0.2	0.2	1.29	1.94	0.336	1.02
4	0.5	0.125	0.2	0.2	0.713	3.51	0.307	1.12
10	0.2	0.05	0.2	0.2	0.445	5.62		
20	0.1	0.025	0.2	0.2	0.445	5.62	0.108	3.18
40	0.05	0.0125	0.2	0.2	0.370	6.76	0.054	6.35

[a] These simulations are presented as a general illustration of the principle. They are not designed to imitate the data presented under Results. In the simulations, B was the only species with absorbance. See Figure 11 for the simulated absorbance/time plots. These plots give rise to two observed rates, k^f_{app} for the fast phase and k^s_{app} for the slow phase of the absorbance changes. [b] The apparent isotope effects listed are obtained by following the normal custom of assuming that a decrease in the fast phase is due to an isotope effect on that phase and a decrease in the slow phase is due correspondingly to a decrease in that phase. In fact, as discussed in the text, a crossover occurs at k_H/k_D of 10 for this set of simulations. The size of the apparent isotope effect, at any give k_H/k_D ratio, will differ from those shown here as the relative initial (proteo) values of k_1, k_{-1}, k_2, and k_{-2} change.

to the prediction of an initial burst as B is converted to D. This burst is especially prominent at high concentrations of S or when k_2 and k_{-2} are fast relative to k_1 and k_{-1}. A burst has even been suggested to be a diagnostic for eq 5 (Strickland et al., 1975). Simulation of the preequilibrium condition yielded rates (after the burst) that fit the predictions described above.

Since the sequence of events in the GAD reaction does not allow for a proper equilibration between species A and B prior to initiating the reaction, it was necessary to explore the effect of starting the reaction without prior equilibration. Simulations of nonequilibrated reactions gave reaction time courses that were nearly monophasic under all conditions. The measured rates from the slower, major phase conformed to the predictions made above.

It is rather unusual in enzymology to find that the apparent rate for a reaction decreases as the substrate concentration increases. Mechanisms to describe such an observation might be expected to be quite complicated. But as we have demonstrated, the simple two-step mechanism of eq 5 will suffice. It is fair, however, to ask whether eq 5 is the simplest mechanism capable of supporting this phenomenon. The only mechanisms simpler than eq 5 are one-step reactions such as eq 7. It can be seen by inspection that eq 7 cannot support

$$A \underset{k_{-1}}{\overset{S,k_1}{\rightleftharpoons}} B \qquad (7)$$

a negative dependence of rate on substrate concentration. As the concentration of S is increased, the apparent rate of formation for B (or decay for A) must increase. Equation 6 represents the complementary two-step mechanism to eq 5. Extensive examination of eq 6 (Strickland et al., 1975; Moore & Pearson, 1981) indicates that increasing the substrate concentration always causes an increase in the apparent rate, up to the point of saturation. We have simulated eq 6 under conditions in which the values of k_{-1}, k_2, and k_{-2} approach the same order of magnitude, situations not addressed by theoretical treatments. Under no conditions have we found the apparent rate to decrease as the substrate concentration is increased. This leaves eq 5 as the simplest mechanism that can support a negative dependence of apparent rate on substrate concentration.

(B) Introduction of an isotope effect into one step of a two-step reversible reaction mechanism (see eq 8) incurs the strong possibility of perturbing the measured rates for both steps. This possibility increases as the values of the measured

$$A \underset{k_{-1}}{\overset{k_1}{\rightleftharpoons}} B \underset{k_{-2}}{\overset{k_2}{\rightleftharpoons}} C \qquad (8)$$

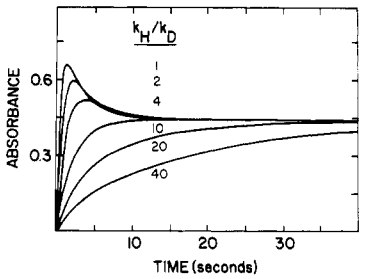

FIGURE 11: Plots of absorbance versus time for simulations of the mechanism in eq 8. Conditions: The starting concentration of A was 10 μM. The extinction coefficients were A, 0, B, 1×10^5 M^{-1} cm^{-1}, and C, 0. Rate constants were k_1 = 2.0, 1.0, 0.5, 0.2, 0.1, or 0.05 s^{-1}, k_{-1} = 0.5, 0.25, 0.125, 0.05, 0.025, or 0.0125 s^{-1}, k_2 = 0.2 s^{-1}, and k_{-2} = 0.2 s^{-1}. The formation of B was monitored. The values for k_1 and k_{-1} were varied in parallel in order to simulate isotope effects on the k_1/k_{-1} step. Isotope effect ratios, $k_H/k_D = 2.0/k_1$, varied from 1 to 40.

rates become more similar. The reason for this is that the measured rates (k^f_{app} and k^s_{app}) for a reversible mechanism represent a complex assemblage of all four intrinsic rate constants, k_1, k_{-1}, k_2, and k_{-2} (Moore & Pearson, 1981). The rigorous mathematical expressions of k^f_{app} and k^s_{app} are

$$k^f_{app} = \{(k_1 + k_{-1} + k_2 + k_{-2}) + [(k_1 + k_{-1} + k_2 + k_{-2})^2 - 4(k_1k_2 + k_{-1}k_{-2} + k_1k_{-2})]^{1/2}\}/2$$

$$k^s_{app} = \{(k_1 + k_{-1} + k_2 + k_{-2}) - [(k_1 + k_{-1} + k_2 + k_{-2})^2 - 4(k_1k_2 + k_{-1}k_{-2} + k_1k_{-2})]^{1/2}\}/2$$

Note that k^f_{app} and k^s_{app} differ only in the sign preceding the square root expression in the above equations.

Let us consider the result of introducing an isotope effect on k_1 and k_{-1}. Perturbing k_1 and k_{-1} would clearly have an effect on both k^f_{app} and k^s_{app}. The apparent rate most intimately associated with k_1 and k_{-1} would be affected most dramatically. If k^f_{app} is the rate most severely affected, it is possible for it to be reduced enough that the associated k^s_{app} could become larger than the observed k^f_{app}.

This is illustrated in Figure 11 and documented in Table III. We have chosen to illustrate the effects on a trace that rises and falls, in order to make the phases more readily distinguishable. Equivalent analyses can be obtained for traces in which both phases proceed in the same direction. These simulations are designed to illustrate a principle. They are not intended to imitate the data presented under Results.

In the above simulations, the intial value (^1H) for k^f_{app} is approximately equal to $k_1 + k_{-1}$, while that for k^s_{app} is generally less than $k_2 + k_{-2}$. As k_1 and k_{-1} are reduced, both measured

rates (k^f_{app} and k^s_{app}) decrease. The amplitude of the slow phase decreases until a point at which only one phase is seen. At still lower values for k_1 and k_{-1}, biphasic traces are again seen. For these latter traces, however, the fast phase is the minor phase. At high k_H/k_D ratios, the measured rate k^f_{app} approaches the true value for k_2 and the measured rate k^s_{app} approaches the true value for k_1. It can be seen that the apparent k_H/k_D ratio, calculated by dividing k^f_{app} (^1H) by k^f_{app} (^2H) or by dividing k^s_{app} (^1H) by k^s_{app} (^2H), does not reflect the actual isotope ratio used in the simulation. For the case illustrated, the apparent isotope ratio for k^f_{app} is seriously underestimated for $k_H/k_D \geq 10$, while that for k^s_{app} is seriously overestimated (especially in view of the fact that no isotope effect occurs in the second step). The quality of this artifact will vary with the mechanism employed. With GAD, we have a rather more complicated system.

From this discussion, it should be clear that considerable confusion can be generated by simply using apparent rates for determining isotope effects in multistep, reversible reaction mechanisms. This is especially likely when the isotope effects involve two protons in the transition state, as is the case with GAD.

References

Alcock, N. W., Benton, D. J., & Moore, P. (1970) *Trans. Faraday Soc. 66*, 2210–2213.

Auer, H. E., & Frerman, F. E. (1980) *J. Biol. Chem. 255*, 8157–8163.

Beaty, N. B., & Ballou, D. P. (1981) *J. Biol. Chem. 256*, 4611–4618.

Beinert, H. (1962) *Methods Enzymol. 5*, 546–557.

Beinert, H., & Page, E. (1957) *J. Biol. Chem. 225*, 479–497.

Beinert, H., & Sands, R. H. (1961) in *Free Radicals in Biological Systems* (Blois, M. S., Brown, H. W., Lemmon, R. M., Lindblom, R. O., & Weissbluth, M., Eds.) pp 17–52, Academic, New York.

Crane, F. L., Mii, S., Hauge, J. G., Green, D. E., & Beinert, H. (1956) *J. Biol. Chem. 218*, 701–716.

Davidson, B., & Schultz, H. (1982) *Arch. Biochem. Biophys. 213*, 155–162.

Dommes, V., & Kunau, W.-H. (1984) *J. Biol. Chem. 259*, 1789–1797.

Entsch, B., Ballou, D. P., & Massey, V. (1976) *J. Biol. Chem. 251*, 2550–2563.

Forsythe, G. E., Malcolm, M. A., & Moler, C. B. (1977) in *Computer Methods for Mathematical Computations*, pp 121–147, Prentice-Hall, Englewood, Cliffs, NJ.

Frerman, F. E., Miziorko, H. M., & Beckmann, J. D. (1980) *J. Biol. Chem. 255*, 11192–11198.

Furuta, S., Miyazawa, S., & Hashimoto, T. (1981) *J. Biochem. (Tokyo) 90*, 1739–1750.

Ghisla, S., Thorpe, C., & Massey, V. (1984) *Biochemistry 23*, 3154–3161.

Gorelick, R. J., Schopfer, L. M., Ballou, D. P., Massey, V., & Thorpe, C. (1985) *Biochemistry 24*, 6830–6839.

Halford, S. E. (1972) *Biochem. J. 126*, 727–738.

Hall, C. L., & Kamin, H. (1975) *J. Biol. Chem. 250*, 3476–3486.

Hall, C. L., & Lambeth, J. D. (1980) *J. Biol. Chem. 255*, 3591–3595.

Hall, C. L., Lambeth, J. D., & Kamin, H. (1979) *J. Biol. Chem. 254*, 2023–2031.

Hauge, J. G. (1956) *J. Am. Chem. Soc. 78*, 5266–5272.

Ikeda, Y., Okamura-Ikeda, K., & Tanaka, K. (1985a) *J. Biol. Chem. 260*, 1311–1325.

Ikeda, Y., Hine, D. G., Okamura-Ikeda, K., & Tanaka, K. (1985b) *J. Biol. Chem. 260*, 1326–1337.

Ikeda, Y., Okamura-Ikeda, K., & Tanaka, K. (1985c) *Biochemistry 24*, 7192–7199.

Kirschner, K., Eigen, M., Bittman, R., & Voight, B. (1966) *Proc. Natl. Acad. Sci. U.S.A. 56*, 1661–1667.

Lau, S.-M., Howell, P., Buettner, H., Ghisla, S., & Thorpe, C. (1986) *Biochemistry 25*, 4184–4189.

Madden, M., Lau, S.-M., & Thorpe, C. (1984) *Biochem. J. 224*, 577–580.

Massey, V., & Ghisla, S. (1974) *Ann. N.Y. Acad. Sci. 227*, 446–465.

Massey, V., & Hemmerich, P. (1978) *Biochemistry 17*, 9–17.

McFarland, J. T., Lee, M.-Y., Reinsch, J., & Raven, W. (1982) *Biochemistry 21*, 1224–1229.

McKean, M. C., Frerman, F. E., & Mielke, D. M. (1979) *J. Biol. Chem. 254*, 2730–2735.

Mizzer, J. P., & Thorpe, C. (1981) *Biochemistry 20*, 4965–4970.

Moore, J. W., & Pearson, R. G. (1981) in *Kinetics and Mechanism*, 3rd ed., pp 296–300, Wiley, New York.

Murfin, W. W. (1974) Ph.D. Thesis, Washington University.

Pohl, B., Raichle, T., & Ghisla, S. (1986) *Eur. J. Biochem. 160*, 109–115.

Reinsch, J., Katz, A., Wean, J., Aprahamian, G., & McFarland, J. T. (1980) *J. Biol. Chem. 255*, 9093–9097.

Reinsch, J., Rojas, C., & McFarland, J. T. (1983) *Arch. Biochem. Biophys. 227*, 21–30.

Schopfer, L. M., & Massey, V. (1979) *J. Biol. Chem. 254*, 10634–10643.

Steyn-Parvé, E. P., & Beinert, H. (1958) *J. Biol. Chem. 233*, 843–852.

Strickland, S., Palmer, G., & Massey, V. (1975) *J. Biol. Chem. 250*, 4048–4052.

Thorpe, C., & Massey, V. (1983) *Biochemistry 22*, 2972–2978.

Thorpe, C., Matthews, R. G., & Williams, C. H., Jr. (1979) *Biochemistry 18*, 331–337.

Thorpe, C., Ciardelli, T. L., Stewart, C. J., & Weiland, T. (1981) *Eur. J. Biochem. 118*, 279–282.

Wenz, A., Thorpe, C., & Ghisla, S. (1981) *J. Biol. Chem. 256*, 9809–9812.

Wenz, A., Ghisla, S., & Thorpe, C. (1985) *Eur. J. Biochem. 147*, 553–560.

Williams, C. H., Jr., Arscott, L. D., Matthews, R. G., Thorpe, C., & Wilkinson, K. D. (1979) *Methods Enzymol. 62*, 185–198.